Journal of Membrane Science 588 (2019) 117220

Contents lists available at ScienceDirect

Journal of Membrane Science

journal homepage: www.elsevier.com/locate/memsci

Mixed-matrix carbon molecular sieve membranes using hierarchical zeolite: A simple approach towards high CO_2 permeability enhancements

Wen Li[a,1], Kunli Goh[b,1], Chong Yang Chuah[a,b], Tae-Hyun Bae[a,b,c,*]

[a] School of Chemical and Biomedical Engineering, Nanyang Technological University, Singapore, 637459, Singapore
[b] Singapore Membrane Technology Centre, Nanyang Technological University, Singapore, 637141, Singapore
[c] Department of Chemical and Biomolecular Engineering, Korea Advanced Institute of Science and Technology, Daejeon, 34141, Republic of Korea

ARTICLE INFO

Keywords:
Hierarchical zeolite 5A
Carbon molecular sieve membrane
CO_2/CH_4 separation
Robeson upper bound
F_{index}

ABSTRACT

Membrane process is a robust technology for CO_2/CH_4 separation. To achieve the energy-efficiency necessary for a cost-effective membrane-based CO_2/CH_4 separation, high-performance membranes are often desirable. There are several approaches that can be undertaken to realize such membranes. In this study, we amalgamated three strategies: 1) filler design optimization by synthesizing hierarchical zeolite 5A comprising micro and mesoporous domains to strengthen the second strategy; 2) mixed-matrix approach by incorporating zeolite fillers to facilitate CO_2 diffusion and reduce transport resistance through a Matrimid® matrix; and 3) membrane carbonization to induce thermal rearrangement, and create free volumes and pore apertures for a faster CO_2 transport. These efforts afforded mixed-matrix carbon molecular sieve membranes with results confirming that our membrane at 30 wt% loading of hierarchical zeolite 5A was able to surpass the 2008 Robeson upper bound limit given a performance of 2450 barrers CO_2 permeability and 19.3 CO_2/CH_4 selectivity. Notably, at this loading, the negative effect brought by the interfacial nanogaps between the filler and carbon matrix diminished, unleashing the potential of the mesopores in facilitating CO_2 diffusion, which led to a two orders of magnitude enhancement in the CO_2 permeability relative to the unfilled carbon molecular sieve membrane. Despite a decrease in the CO_2/CH_4 selectivity, the hierarchical zeolite 5A is effective in alleviating the intensity of the permeability-selectivity trade-off. Also, benchmarking of the filler effectiveness is first demonstrated using a new filler enhancement index, F_{index}. The largest F_{index} value in this study was 1.97. This attaches a label of "competent" to our hierarchical zeolite 5A filler at 30 wt% loading, demonstrating the success of our strategies.

1. Introduction

Natural gas and biogas, which consist of methane gas (CH_4), are important energy resources for relieving our reliance on fossil fuels. To fully capitalize on CH_4 as an alternative fuel, enriching the CH_4 content by separating carbon dioxide (CO_2) gas in natural gas and biogas is critical. For this purpose membrane-based technology offers strong advantages such as safe operation, energy-efficiency, cost-effectiveness alongside small plant footprint to stay competitive against conventional technologies, which include physical and chemical scrubbing as well as pressure swing adsorption [1]. Polymeric membranes [2,3] are by far the most commonly used membrane materials for many gas separation processes, including hydrogen purification, biogas upgrading and air separation [4,5], due to their well-established industrial fabrication methods and high cost-competitiveness as compared to other materials (*e.g.* inorganic materials) [6,7].

One of the biggest issues with polymeric membranes is their recurrent permeability-selectivity trade-off [8] driven by a solution-diffusion transport mechanism within the dense structure of the membranes. As this is a limitation inherent to the polymers used, efforts to alleviate the issue are usually materials-oriented [9]. Among these efforts, thermal treatment is a process to decarboxylate polymer precursors at high temperatures. During the process, the structure of the polymer chains changes, disrupting the polymer's rigidity [10] and creating fractional free volumes which comprise cavities and constrictions that allow discrimination of gas molecules based on their kinetic diameters. The resulting membranes, termed as carbon molecular sieve membranes (CMSMs) due to the highly graphitic domains after carbonization [11], usually exhibit substantial improvement in gas permeability without sacrificing on the membrane selectivity [12], making

* Corresponding author. School of Chemical and Biomedical Engineering, Nanyang Technological University, Singapore, 637459, Singapore.
E-mail address: thbae@kaist.ac.kr (T.-H. Bae).
[1] These authors contributed equally to this work.

https://doi.org/10.1016/j.memsci.2019.117220
Received 5 March 2019; Received in revised form 19 June 2019; Accepted 27 June 2019
Available online 28 June 2019
0376-7388/

them highly versatile for separating a wide range of gas pairs, like CO_2/CH_4 separation, air and hydrocarbons separation.

The permeability-selectivity trade-off is clearly demonstrated in Robeson plots (log-log plots of permeability against selectivity) where an upper bound limit is defined to highlight the best performances from polymeric membranes. To drive CMSMs to surpass this upper bound, researchers have to optimize several carbonization conditions, including the atmospheric environment (He, Ar, N_2, CO_2, vacuum), heating rate, thermal soak time and pyrolysis temperature (500–1000 °C) [13,14]. For instance, administering a He environment can increase CO_2 permeance but leads to a significant loss in CO_2/CH_4 selectivity while that of an Ar environment tends to result in an increase in the gas selectivity of CMSMs. A higher pyrolysis temperature is also known to produce CMSMs of higher density and compactness [13]. Despite this, carbonization conditions are not always generalizable to all types of precursor polymers. As such, researchers are required to carry out painstaking optimization on a case-by-case basis. Alternatively, high-performance CMSMs can be realized from precursor polymers with outstanding intrinsic separation capacities, such as the highly permeable/selective 6FDA-based polymers [13]. However, such precursor polymers are more highly priced compared to zeolites and commercial polymers (Matrimid®). In addition, to successfully prepare 6FDA-TMPDA polyimide polymer, every step during the synthesis needs to be carefully carried out, as described in our previous work [15]. For instance, the requirement for monomers purification before the reaction, synthesis procedures to be kept under inert environment as well as complete removal of residual solvents within products are essential steps affecting the quality of the precursors. Overall, apart from economic consideration, such laborious and more complex synthesis methods are critically stifling the commercial potential of such high-performance polymer precursors.

To close these technological gaps, we adopted a simple approach to elevate the separation performances of CMSMs. The approach involves amalgamating CMSM fabrications with a mixed-matrix approach, where porous filler materials are incorporated within the carbon graphitic domains to either create low-resistance transport pathways or serve as barriers to impede the less permeable gas molecules [16]. To date, filler materials such as mesoporous carbon [17], SBA-15 and MCM-48 [18], as well as zeolite T [19], zeolite KY [20] and zeolite L [21] have been utilized to create either enhancements in CO_2 permeability and/or CO_2/CH_4 selectivity of CMSMs. Apart from this approach, we also strategize on filler design optimization to further drive the CO_2/CH_4 separation performances beyond the upper bound limit. Hence, we selected Matrimid® 5218 polyimide and zeolite 5A as the precursor polymer and filler material, respectively, to realize our mixed-matrix CMSM design. Matrimid® 5218 was chosen because of its commercial availability, cost-competitiveness as well as its high intrinsic CO_2/CH_4 selectivity of 37.5 under the measurement conditions of 35 °C and 2 bar feed pressure [22]. Zeolite 5A, on the other hand, is a classical filler material which possesses molecular channels and rigid cavities that can provide optimized free spaces and void volumes for effective gas transport, especially CO_2 [23,24]. It is worth noting that, as compared to 4A which is the original form containing Na^+ as the counter cation, 5A zeolite possessing Ca^{2+} as the counter cation allows a much faster CO_2 diffusion as evidenced by the CO_2 adsorption study (Fig. S3). The previous studies also reported that the CO_2 permeability of 4A zeolite is less than 10 barrer, indicating that 4A zeolite is not effective in improving the CO_2 permeability of CMSM which is much higher than 10 barrer [9,25,26]. More importantly, the pore structure of zeolite 5A can be easily optimized by tuning with the aid of a pore expanding agent, leading to a hierarchical structure with both meso and micropores. Comparing this filler to bulk zeolite 5A with mono-micropores, the presence of mesopores in hierarchical zeolite 5A (H-zeolite 5A) creates more open channels for CO_2 transport.

For this reason, we optimized our CMSMs from Matrimid® precursor incorporating H-zeolite 5A (LTA topology) filler. Our results demonstrate that the H-zeolite 5A is indeed highly effective in enhancing the CO_2 permeability, which helps to moderate the adverse effects brought by the permeability-selectivity trade-off. In particular, at 30 wt % H-zeolite 5A loading, our membrane was able to achieve a two orders of magnitude enhancement in the CO_2 permeability compared to the unfilled CMSM. A filler enhancement index, F_{index}, was also used to evaluate the effectiveness of our H-zeolite 5A [27], benchmarking the filler as “competent” at a loading of 30 wt%. Effectively, our strategy was successfully demonstrated as the performance of our mixed-matrix CMSM surpassed the 2008 Robeson upper bound limit.

2. Experimental

2.1. Materials

Sodium metasilicate pentahydrate (≥95.0%), sodium hydroxide (≥98.5%), sodium aluminate (Al: 50–56%; Na: 37–45%), dimethyloctadecyl[3-(trimethoxysilyl)propyl]ammonium chloride solution (TPOAC, 42 wt% in methanol) and calcium nitrate tetrahydrate ($Ca(NO_3)_2$) were purchased from Sigma-Aldrich, Merck. Chloroform (≥99.8%) was purchased from VWR. The reagents and solvent were used as-received. Matrimid® 5218 was purchased from Ciba Specialty Chemicals and was dried in vacuum oven at 180 °C overnight prior to use.

2.2. Synthesis of bulk and hierarchical zeolite 5A

Bulk and H-zeolite 5A were synthesized as described in the literature [28]. For H-zeolite 5A (with both microporous and mesoporous domains), the precursor gel with a molar ratio of 10 Al_2O_3/40 Na_2O/15 SiO_2/2400 H_2O/1.25 TPOAC were prepared at room temperature. In separate polypropylene bottles, one solution containing sodium metasilicate pentahydrate, sodium hydroxide, TPOAC and deionized (DI) water was mixed, while another solution comprising sodium aluminate dissolved in DI water was separately prepared. After the solutions were strongly agitated for 2 h, both solutions were mixed and heated at 100 °C for 4 h. Upon completion of reaction, the products were collected via vacuum filtration, which were then washed with copious amount of DI water to remove unreacted raw materials and impurities. The resulting products were dried at 100 °C overnight in a convection oven, followed by calcination at 550 °C for 3 h in a furnace at a heating rate of 1 °C/min. This step helped to remove TPOAC that was present in the mesopores, affording hierarchical zeolite 4A. In the following step, Na^+ cations in LTA zeolite domains (zeolite 4A) was replaced with Ca^{2+} cations using ion-exchange to yield zeolite 5A. Briefly, 1 g of zeolite 4A was first dispersed in 50 mL of 0.5 M $Ca(NO_3)_2$ solution before vigorous stirring at 60 °C for 12 h. This ion-exchange procedure was repeated once more to ensure a higher degree of substitution to Ca^{2+}. The H-zeolite 5A was obtained by filtering the product solution and drying at 80 °C for 24 h. On the other hand, the synthesis of bulk zeolite 5A (with only microporous domains) was prepared using the same procedure as hierarchical zeolite 5A except without the addition of TPOAC. The molar ratio of the precursor gel for bulk zeolite 5A was 10 Al_2O_3/40 Na_2O/15 SiO_2/2400 H_2O.

2.3. Synthesis of mixed-matrix carbon molecular sieve membranes

The synthesis of CMSMs was summarized in Scheme 1. Polymeric flat sheet precursor membranes were fabricated using a solution-casting technique as reported elsewhere [29,30]. For the synthesis of polymeric mixed-matrix membranes containing bulk and H-zeolite 5A (10, 20 and 30 wt%), the fillers were first ground and dispersed in chloroform with the aid of a sonication horn (Qsonica, Q125) to obtain a homogeneous dispersion. Next, Matrimid® powder was incorporated into the suspension, followed by vigorous stirring until the polymer was dissolved completely. The viscosity of the dope solution was controlled by fixing

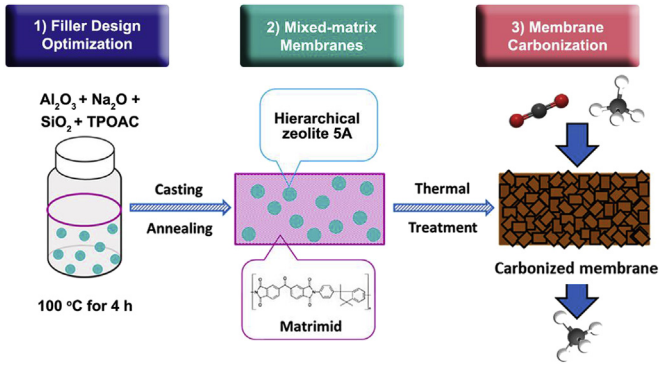

Scheme 1. Synthesis procedure of carbon molecular sieve membranes [31].

the concentration of Matrimid® in the range of 10–15 wt%. Flat sheet membranes were cast onto a glass plate with a casting knife in a glove bag that was filled with chloroform vapor to slow down the solvent evaporation time. Upon phase inversion, the membranes were annealed at 180 °C overnight to remove any residual solvents. The precursor membranes then underwent a carbonization process in a tube furnace (Carbolite GERO, CTF 12/100/900). Ar gas (purity of 99.9995%, Airliquide) was first purged into the quartz tube for approximately 1 h to create an inert environment and to remove any residual air and moisture that could potentially trap inside the tube. Following, the membrane precursors were treated via a two-step ramp-dwell profile comprising 380 °C heating for 30 min at a rate of 2 °C/min and 550 °C heating for 2 h at a rate of 0.5 °C/min. After completion, the carbonized membranes were cooled to room temperature before storing them for future performance evaluations and characterization.

2.4. Materials and membranes characterization

Powdered X-ray diffraction (PXRD) patterns of zeolites, precursor membranes and CMSMs were measured with a Bruker D2 phaser diffractometer equipped with a Cu Kα source in the 2θ range of 5–50°. Thermal stabilities of zeolites and precursor membranes were determined using a thermogravimetric/differential thermal analyzer (TGA, SDT Q600 TA Instrument). The experiments were operated under N_2 purging at 100 ml/min, with a heating rate of 10 °C/min and temperature ranging from 50 to 900 °C. The morphologies of zeolites, precursor membranes and CMSMs were observed using a field emission-scanning electron microscope (FE-SEM, JSM6701 JOEL). To preserve the cross-sectional morphologies, the samples were first cryogenically fractured in liquid nitrogen prior to gold coating. The particle size distribution of zeolites was measured via dynamic light scattering (DLS, BIC PALS ZetaSizer). N_2 physisorption at −196 °C (77 K) and a P/P_o range of 0–1 bar (Autosorb 6B, Quantachrome) was used to evaluate the porosity properties of both bulk and H-zeolite 5A. The samples were first activated at 250 °C for 24 h under high vacuum prior to the measurement and the mesopore size distributions were determined from a Barrett-Joyner-Halenda (BJH) algorithm. On the other hand, CO_2 and CH_4 adsorption isotherms were acquired via a volumetric gas sorption analyzer (iSorb HP1, Quantachrome) under a pressure range of 0–1 bar. The measurements were conducted at a controlled temperature of 35 °C using a water circulator.

2.5. Mixture gas permeation evaluations

Mixture gas permeation tests were conducted using a constant pressure-variable volume system (GTR Tec Corporation). The CO_2/CH_4 (50/50) mixture and helium (He, purity of 99.9995%) gases used in the system were purchased from Airliquide. Membranes were first mounted onto a permeation cell before exposing to continuous flow of He and CO_2/CH_4 mixture gas on the down and upstream sides at a feed and permeate pressure of 1 bar, respectively. The temperature of the permeation cell was set at 35 °C. At a specific time interval, the downstream gas was swept by He until the concentration of the permeating gas remained unchanged. The CO_2 and CH_4 concentration of the permeate gas were calculated from the gas chromatogram. Each permeation measurement was repeated at least three times for both precursor membranes and CMSMs to ensure reproducibility in the results. In this work, our goal was to investigate the improved separation performance of CMSMs for specifically biogas upgrading. Although there exist negligible amount of other gases, biogas mainly consists of CH_4 (60–70 vol%) and CO_2 (30–40 vol%) [27]. Therefore, a mixture gas of CO_2/CH_4 (50/50) applied in this work was representative of the biogas composition.

Based on the separation performances obtained, a filler enhancement index, F_{index}, was calculated for each mixed-matrix CMSM using the following equation:

$$F_{index} = \ln\left(\frac{P_{filled}}{P_{unfilled}}\right) + \eta\ln\left(\frac{\alpha_{filled}}{\alpha_{unfilled}}\right) \quad (1)$$

where P_{filled} and $P_{unfilled}$ refer to the CO_2 permeability while α_{filled} and $\alpha_{unfilled}$ are the CO_2/CH_4 selectivity of the mixed-matrix and unfilled CMSMs, respectively, and η is an enhancement coefficient of value 2.636, which stems from the slope of the 2008 Robeson upper bound. The F_{index} was empirically developed to evaluate the effectiveness of fillers in enhancing the separation performance of mixed-matrix membranes [27], which we utilized here to help us understand the effects brought by the bulk and H-zeolite 5A fillers.

3. Results and discussion

3.1. Properties of bulk and hierarchical zeolite 5A

Fig. 1(a) and (b) illustrated the overall morphologies of zeolite 5A, showing uniform structures for both bulk (cubic) and H-zeolite 5A (spherical). The particle size of bulk and H-zeolite 5A was estimated from the FE-SEM images to be around 2–3 μm and 6–7 μm respectively. These results were also verified via DLS analysis as illustrated in Fig. S1. It is noteworthy that we were unable to control the size of H-zeolite 5A due to its complicated reaction system. Thus, we intentionally chose this large 5A bulk zeolite particle, which is the largest one among the samples we successfully synthesized previously (ranged from 300 nm to 2–3 μm) [28,32,33], to minimize the effect of particle size on membrane performance. Next, successful synthesis of bulk and H-zeolite 5A was verified by PXRD. As shown in Fig. 1(c), the characteristic peaks of both zeolites resemble the XRD patterns as those reported in the literature [28]. Noteworthy of mentioning is the lower peak intensities of H-zeolite 5A as compared to the bulk zeolite 5A. The determination of relative crystallinity in XRD patterns is based on the relative intensity of specific peaks. As described in Fig. 1 (c), the characteristic peak located at $2\theta = 7.6°$ of H-zeolite 5A was much lower and the ratio of peak intensity was around 0.283 as compared to zeolite 5A. This phenomenon suggested a lower crystallinity of H-zeolite 5A probably because of the presence of mesoporosity, which leads to a lower fraction of zeolitic domains. To determine the suitability of the zeolites for the subsequent carbonization process, the thermal stabilities were evaluated from 50 to 900 °C (Fig. 1 (d)). Based on the TGA profile, a continuous weight loss (c.a. 15–20%) up to 220 °C was observed for both bulk and H-zeolite 5A, which we attributed to the presence of moisture inside the pores. After heating beyond 220 °C, all moisture was removed and further weight loss was not observed for both zeolites even at a temperature as high as 900 °C. This suggests that both zeolites are capable of retaining their crystallinity and pore structures in the Matrimid® matrix after carbonization at 550 °C.

Porosity properties of both bulk and H-zeolite 5A were quantified using N_2 physisorption isotherm at −196 °C (77 K) and P/P_o range from

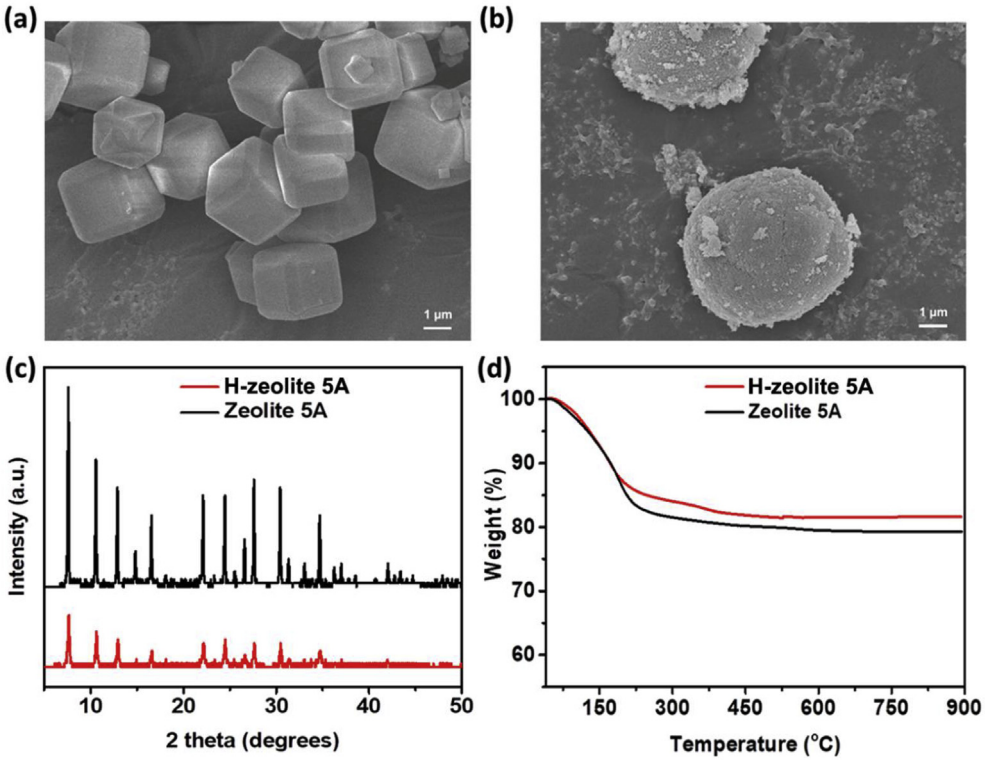

Fig. 1. Field emission-scanning electron microscope (FE-SEM) morphologies of (a) bulk and (b) H-zeolite 5A; (c) Powder X-ray diffraction (PXRD) patterns of bulk and H-zeolite 5A; (d) Thermogravimetric analysis (TGA) curves of bulk and H-zeolite 5A from 50 to 900 °C.

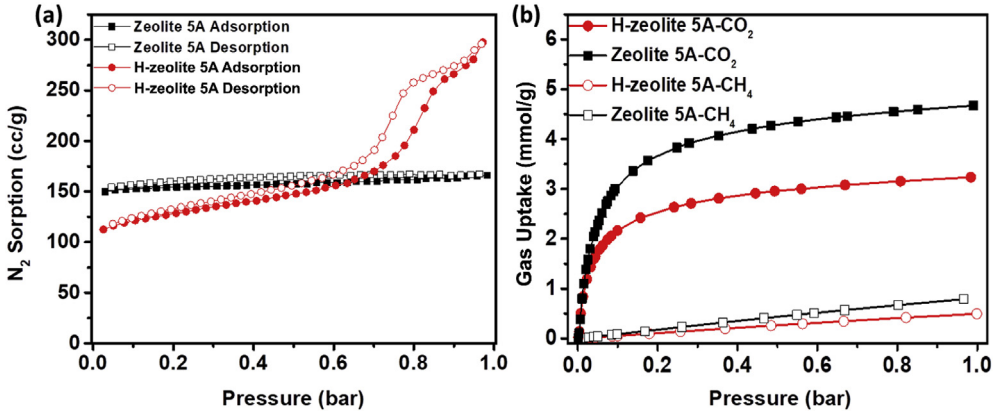

Fig. 2. (a) N_2 physisorption isotherms of bulk and H-zeolite 5A measured at −196 °C (77 K) under the P/P_o range of 0–1 bar; (b) CO_2 and CH_4 adsorption capacities of bulk and H-zeolite 5A at 35 °C from 0 to 1 bar.

0 to 1 bar (Fig. 2(a)). In general, both bulk and H-zeolite 5A demonstrated high N_2 sorption at low P/P_o values, indicating the presence of large micropore volumes. While the H-zeolite 5A exhibited lower N_2 sorption compared to the bulk zeolite 5A at low P/P_o values, the presence of a hysteresis loop between the adsorption and desorption curves showed the existence of mesopores. As demonstrated in Fig. S2, the mesopore sizes of both H-zeolite 4A and 5A were determined by a BJH algorithm [34] to be around 6.9 and 8.5 nm, respectively, providing evidence that the pore size was expanded after ion-exchange of Na^+ with Ca^{2+}. Based on the N_2 physisorption isotherms, surface area as well as the micropore surface area and micropore volume were computed using the Brunauer–Emmett–Teller (BET) theory, Langmuir equation and t-plot method, respectively. Our results show that the surface area and micropore volume of H-zeolite 5A are found to be slightly lower than that of the bulk zeolite 5A, indicating a lower crystallinity which is most likely due to the presence of mesoporosity (Table S1).

Next, pure component CO_2 and CH_4 adsorption of bulk and H-zeolite 5A were investigated to evaluate their affinities towards these gases. A close analysis of Fig. 2(b) shows a rapid CO_2 adsorption at low CO_2 partial pressures for both zeolites. This suggests the existence of favorable interactions between CO_2 molecules and active sites in the zeolitic frameworks as facilitated by induced dipole-dipole interaction and driven by a stronger polarizability (29.11×10^{-25} cm^3 vs. 25.93×10^{-25} cm^3) and quadrupole moment (4.30×10^{-26} esu cm^2 vs. 0 esu cm^2) of CO_2 as compared to CH_4 molecules. At increasing CO_2 partial pressure, both zeolites starts to show a gradual saturation of the CO_2 adsorption with increasing feed pressure. CH_4 adsorption, on the other hand, exhibits a linear CH_4 isotherm, indicating a weaker affinity of the CH_4 molecules towards both zeolites. A weaker CO_2 and CH_4 adsorption of the H-zeolite 5A as relative to the bulk zeolite 5A also implies a slight decrease in the number of active sites as a result of the

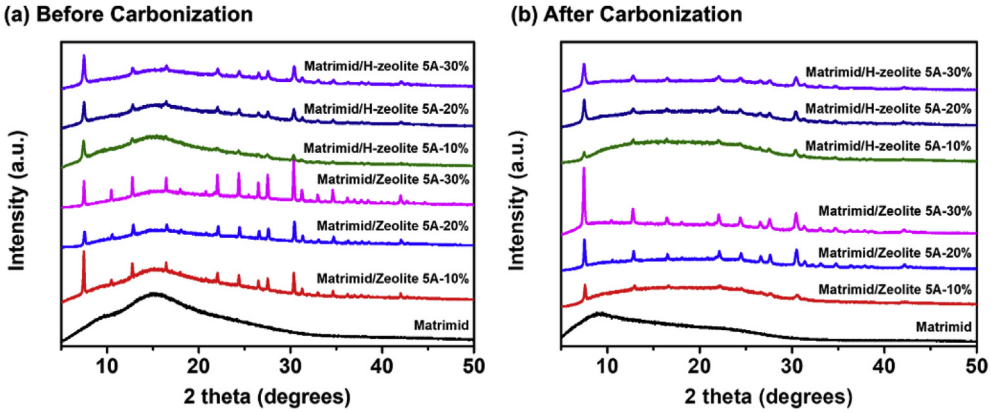

Fig. 3. X-ray diffraction (XRD) patterns of pure Matrimid® membrane and mixed-matrix carbon molecular sieve membranes (a) before and (b) after carbonization.

introduction of mesoporous domains in the zeolitic framework of H-zeolite 5A.

3.2. Properties of precursor and carbon molecular sieve membranes

Characterization of the as-prepared membranes is evaluated from three aspects, namely, thermal stability, structural intactness, and membrane integrity. Previously, the thermal stability of the zeolite 5A was demonstrated by heating up to 900 °C without showing signs of structural degradation (Fig. 1 (d)). Similarly, the same was observed when the zeolites were incorporated into the membrane matrix as evidenced by the TGA results represented in Fig. S4. At a temperature of 520 °C, the substantial weight loss observed by all membranes, including the unfilled Matrimid®, suggests that the polymer starts to undergo thermal rearrangement and carbonize at this temperature. In this regard, we have chosen a slightly higher carbonization temperature at 550 °C. The thermal stability of the zeolite 5A after incorporating into membrane matrix is also apparent from the PXRD results. Particularly, membranes comprising bulk and H-zeolite 5A shows characteristic peaks of zeolite 5A, suggesting that the crystallinity of the zeolitic domains remain intact after carbonization (Fig. 3). In fact, throughout the process of carbonization, the most significant change only happens to the Matrimid® matrix as corroborated by a shift in the broad XRD peak of the Matrimid® matrix from $2\theta = 16^{\circ}$ to a lower angle of $2\theta = 9^{\circ}$ (Fig. 3). Structurally, this implies an increase in the d-spacing (fractional free volume) as the nature of the matrix changes from polymeric to carbon [35,36], which has important implications for the membrane performances.

The interfacial morphologies of CMSMs after zeolite 5A incorporation were observed by probing the membrane cross-sectional morphologies using FE-SEM. Critically, the mixed-matrix precursor membranes displayed clear defects before carbonization. These defects appeared in the form of *sieve-in-a-cage* morphologies as exemplified by the presence of voids at the polymer/zeolite interfaces (Fig. S5). *Sieve-in-a-cage* morphologies are reportedly due to the poor interfacial compatibility between the zeolite 5A and Matrimid® matrix, which is a common challenge arising from pairing an inorganic filler with an organic polymeric material [16,32]. However, after carbonization, the interfacial voids between the zeolite 5A and carbon matrix were seemingly narrowed (Fig. 4). We believe that the glassy Matrimid® polymer matrix became rubbery as it reached its glass transition temperature, T_g, of 319 °C during carbonization [37]. This rendered the polymer chains enough flexibility to close up the interfacial voids before matrix carbonization occurred at a higher temperature. Nevertheless, while no visible voids are observed under FE-SEM (Fig. 4), we remain doubtful on the complete sealing of the interfacial voids. Realistically speaking, there is a possibility that microscopically invisible nanogaps may continue to linger at the carbon/zeolite interfaces, which we will provide evidence in the next section.

It is well-known that a major disadvantage that hinders the practical applications of CMSMs is their poor mechanical stability. To date, several researchers have attempted to improve the mechanical properties of CMSMs. For instance, Yoshimune and Haraya et al. introduced sulfonic groups into polyimide polymer and obtained a more flexible carbon hollow fiber membrane with a small radius [38]. In addition, Ismail et al. claimed that the utilization of polyacrylonitrile (PAN) as a precursor, which was widely applied in high strength carbon fiber, was feasible in minimizing brittleness [39]. However, the mechanical stability remains dramatically influenced by factors such as pyrolysis temperature [13]. In this work, the mechanical properties of our CMSMs are comparably brittle, making accurate evaluation using typical measurements extremely challenging. Hence, further studies on the effect of filler loadings on the mechanical properties of mixed-matrix CMSMs will be an interesting follow-up topic to be pursued by unconventional methods.

3.3. CO_2/CH_4 separation performance of precursor and carbon molecular sieve membranes

To substantiate our deductions in characterization and verify the success of our strategy used in membrane design, we next evaluate the separation performances of our CMSMs under mixture gas permeation conditions. The CO_2 permeability and CO_2/CH_4 selectivity of unfilled Matrimid® precursor membrane were reported as 11 barrers and 36.7, respectively (Table 1). These values are comparable with data reported in the literature (10.2 barrers and 33.6 selectivity) which was measured under similar conditions of 40 °C and 1 bar pressure using 50:50 CO_2/CH_4 mixture [32]. Upon carbonization, the unfilled Matrimid® CMSM reported an enhanced CO_2 permeability of 29 barrers and 49.2 CO_2/CH_4 selectivity (Table 1). As previously mentioned in our interpretation of the d-spacing of the Matrimid® matrix (Fig. 3), this enhancement in separation performance can be attributed to the increase in the fractional free volume brought by the thermal rearrangement of the matrix during carbonization. Without carbonization, enhancement in separation performances can also be achieved by incorporating bulk and H-zeolite 5A fillers into polymeric Martimid® membranes. While the outcome of this standalone mixed-matrix approach is positive, the obtainable enhancement in performance is limited and insufficient for achieving our goal of surpassing the 2008 Robeson upper bound limit [8].

For this reason, we have adopted to combine a mixed-matrix approach with a membrane carbonization strategy. The incorporation of bulk and H-zeolite 5A into the carbon matrix has seen the CO_2 permeability of the mixed-matrix CMSMs demonstrating a different extent of increment with increasing filler loading. With bulk zeolite 5A, the CO_2 permeability was enhanced above 3000% as filler loading increases

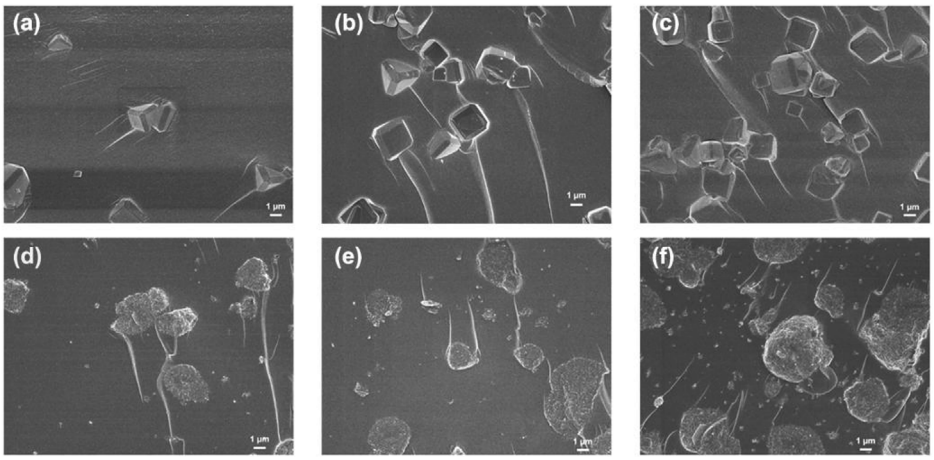

Fig. 4. Cross-sectional field emission-scanning electron microscope (FE-SEM) morphologies of carbon molecular sieve membranes with (a) 10 wt%, (b) 20 wt%, and (c) 30 wt% bulk zeolite 5A, as well as (d) 10 wt%, (e) 20 wt%, and (f) 30 wt% H-zeolite 5A fillers.

from 10 to 30 wt%. With H-zeolite 5A, we observed an exceptional two orders of magnitude enhancement, reaching a high CO_2 permeability of 2450 barrers (Table 1). To determine the origin of these enhancements, we examined the CO_2/CH_4 selectivity of these membranes. Firstly, a decrease in the selectivity of about ~48% was observed with 10 wt% loading of each type of zeolite 5A. This was followed by another ~20% decrease in the selectivity as the loading increased to 20 wt% before stabilizing considerably at 30 wt% (Table 1). These results corroborate our deductions in FE-SEM characterization, which suggest that narrow nanogaps continue to remain at the carbon/zeolite interfaces after carbonization, leading to a decrease in the selectivity as loadings increased. The impact caused by these nanogaps, however, weakens as the loading enters the region of 20–30 wt%. At a loading of 30 wt%, the pore size effect arising from zeolite 5A becomes apparent. Matrimid®/H-zeolite 5A-30% was able to maintain an almost comparable selectivity as Matrimid®/Zeolite 5A-30% (Table 1), suggesting that the presence of mesopores in the filler exert a nominal impact on the selectivity of the CMSMs. More importantly, the mesopores serve with great capacity as transport pathways supplementary to the intrinsic micropores of zeolite 5A. This is evidenced by the 1.6-folds strong enhancement in the CO_2 permeability as we compare the performance of Matrimid®/Zeolite 5A-30% to Matrimid®/H-zeolite 5A-30% (Table 1).

In general, the particle sizes, shapes and even degree of crystallinity of fillers would influence the integrity of the mixed-matrix membranes, leading to different gas transport properties. For instance, based on the FE-SEM images in Fig. 1 (a) and (b), the shape of the H-zeolite 5A was spherical, resembling that of the cubic zeolite 5A. Hence the impact of the particle shape would be minor, especially compared to the effect of pore size. Besides, the crystallinity degree of H-zeolite 5A was lower than that of bulk zeolite 5A as described in Fig. 1 (c). In this case, a smaller improvement in the separation performance was expected by the filler with a lower crystallinity. However, with the addition of H-zeolite 5A, a much better CO_2/CH_4 separation performance was obtained, indicating that the influence of pore size was again more important than the degree of crystallinity. Furthermore, we have tried to make a comparison of the performances of other mixed-matrix CMSMs as summarized in Table S2. While some papers reported significant enhancement of CO_2/CH_4 selectivity, our enhancement in CO_2 permeability remains outstanding among these works, despite a considerable drop in the CO_2/CH_4 selectivity. Nevertheless, such a comparison is not entirely unbiased. As depicted in Table S2, different membrane configurations, different filler types/loadings, different polymer matrices as well as testing conditions were reported. Hence, benchmarking membrane performances by a sheer comparison of absolute values are not sufficient in understanding filler effectiveness in the carbon matrix.

3.4. Benchmarking performances to Robeson upper bound and F_{index}

Up to now, our analysis appears to demonstrate the success of our strategy in using filler design optimization alongside membrane carbonization to realize high CO_2/CH_4 separation performances. To attest this claim, we carry out benchmarking analysis to evaluate the positioning of our membranes performances (Fig. 5(a)). As observed in the literature, it is generally challenging for current performance of CMSMs to surpass the 2008 upper bound limit except for one that was derived from an in-house made 6FDA/BPDA-DAM polymer, which is costly to

Table 1
Mixed gas permeation results measured at 35 °C and 1 bar upstream pressure (CO_2/CH_4 = 50/50) and F_{index} values for Matrimid® precursor membrane as well as unfilled Matrimid® and mixed-matrix carbon molecular sieve membranes.

Carbonization	Membrane	CO_2 permeability[a] (barrer)	CO_2/CH_4 selectivity[b]	F_{index}[c]
Before	Matrimid®	11 ± 0	36.7 ± 1.3	–
After	Matrimid®	29 ± 1	49.2 ± 2.0	–
	Matrimid®/Zeolite 5A-10%	233 ± 2	26.3 ± 0.3	0.43
	Matrimid®/Zeolite 5A-20%	473 ± 19	20.5 ± 0.2	0.48
	Matrimid®/Zeolite 5A-30%	951 ± 3	23.0 ± 0.2	1.49
	Matrimid®/H-zeolite 5A-10%	704 ± 17	24.9 ± 0.5	1.39
	Matrimid®/H-zeolite 5A-20%	967 ± 24	19.7 ± 0.1	1.09
	Matrimid®/H-zeolite 5A-30%	2450 ± 40	19.3 ± 0.1	1.97

[a] 1 barrer = $10^{-10}.\frac{cm^3_{STP}\cdot cm}{cm^2\cdot S\cdot cmHg}$

[b] Ratio of CO_2 permeability over CH_4 permeability.

[c] Based on statistical analysis of 470 fillers in the literature, fillers having different F_{index} values are classified into 5 labels, namely, 1: ideal (> 8.00), 2: exemplary (8.00–4.00), 3: competent (4.00–1.50), 4: moderate (1.50–0.00) and 5: incompetent (< 0.00) [27].

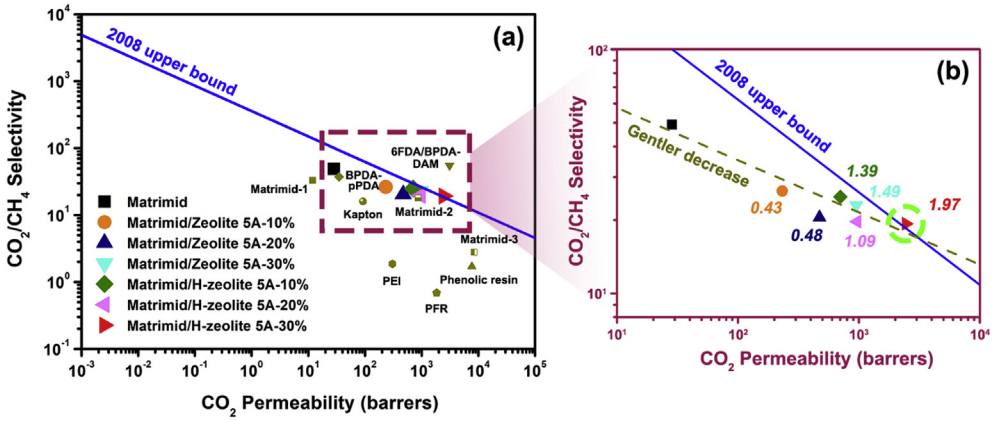

Fig. 5. (a) Robeson plot comparing CO_2 permeabilities and CO_2/CH_4 selectivities of carbon molecular sieve membranes used in this work and those reported elsewhere. Matrimid®-1: 25 °C, 1 bar, CO_2/CH_4 = 10/90 [40]; Matrimid®-2: 35 °C, 10 bar, pure gas [41]; Matrimid®-3: 40 °C, pure gas [42]; Kapton®-1: 25 °C, 1 bar, CO_2/CH_4 = 10/90 [40]; PEI (polyetherimide): 25 °C, 2 bar, pure gas [43]; PFR (phenol–formaldehyde resin): 20 °C, pure gas [44]; Phenolic resin: 20 °C, pure gas [45]; 6FDA/BPDA-DAM: 22 °C [46]; BPDA-pPDA: 25 °C, pure gas [47]. (b) The separation performances reported in this study, showing clearly a gentler decrease in the slope (dotted line), which suggests a trade-off of less intensity. The F_{index} values of our mixed-matrix carbon molecular sieve membranes are included here. It is interesting to note that as the membrane performances approach or exceed the upper bound limit, the F_{index} values increase accordingly.

synthesize and has little commercial value. On the other hand, in this work, the Achilles heel of our mixed-matrix CMSMs is in the permeability-selectivity trade-off as presence of interfacial nanogaps tend to reduce the membrane selectivity up to a filler loading of 20 wt%. This impact, however, diminishes at 30 wt% filler loading. At this specific loading, the positive effect from the mesopores in H-zeolite 5A emerges and drives the performance of Matrimid®/H-zeolite 5A–30% to hit or slightly surpass the 2008 upper bound limit (Fig. 5(a)). In this regard, it is important to emphasize that, while our strategy is unable to completely reverse the trade-off phenomenon, the strong enhancement in CO_2 permeability by 30 wt% loading of H-zeolite 5A in the carbon matrix is able to alleviate the intensity of the trade-off as exemplified by a gentler decrease in the performance of our CMSMs shown in the Robeson plot (dotted line in Fig. 5(b)). Such an assessment would more accurately reflect the impact resulting from our strategy.

We also contemplated with the F_{index} as a means to measure the effectiveness of our H-zeolite 5A when loaded at 30 wt% in the carbon matrix. The F_{index} is an empirical rating metric, which was recently developed by our group to evaluate filler effectiveness [27]. Owing to the fact that most mixed-matrix membranes have performances governed strongly by the intrinsic separation properties of the polymer matrices, performance benchmarking by the Robeson upper bound is insufficient to showcase the filler effectiveness. Hence, we empirically arrive at a F_{index}, which downplays the matrix effect to highlight the filler effectiveness. This is achieved by normalizing the permeability and selectivity terms as highlighted in eq (1). By taking into account both the permeability and selectivity enhancements, the F_{index} is aimed at providing a single rating that can accurately measure the effectiveness of the filler irrespective of the matrix it is incorporated into. The formula (eq (1)) has an extra weighting (designated as η) tagged on the selectivity enhancement term to emphasize the importance of upholding the selectivity of mixed-matrix membranes as well as to credit fillers that are capable of enhancing membrane selectivity with a higher F_{index} value. In view of this, we calculated the F_{index} values of all mixed-matrix CMSMs. Generally, the F_{index} values increase as membrane performances approach the upper bound limit. When the performance of Matrimid®/H-zeolite 5A–30% exceeded the upper bound, the F_{index} gave the highest value at 1.97 (Fig. 5(b)). This suggests that at 30 wt% loading the H-zeolite 5A is effective in elevating the performance of the CMSM despite experiencing a significant drop in the CO_2/CH_4 selectivity (Table 1). Based on our statistical analysis of 470 fillers, a F_{index} value of 1.97 would make H-zeolite 5A at 30 wt% loading eligible for the "competent" filler label while the bulk zeolite 5A or H-zeolite 5A at lower loadings could only settle for an inferior "moderate" label (Table 1) [27]. Accordingly, the two orders of magnitude enhancement in the CO_2 permeability, enabled only by H-zeolite 5A at 30 wt% loading, overwhelmingly nullify the negative impact brought by the decrease in selectivity and compellingly push the F_{index} value into range of "competent" filler label.

4. Conclusion

In this study, we have successfully demonstrated the strategy of filler design optimization with membrane carbonization to realize mixed-matrix carbon molecular sieve membranes incorporating hierarchical zeolite 5A filler. The hierarchical filler not only possesses intrinsic micropores but also mesopores of ~8 nm to offer additional transport pathways to facilitate CO_2 diffusion through the carbon matrix of the membranes. For these reasons, a strong enhancement in the CO_2 permeability of two order of magnitude was observed when 30 wt % loading of the hierarchical zeolite 5A filler was incorporated into the carbon molecular sieve membrane. Despite a decrease in the CO_2/CH_4 selectivity due to the presence of nanogaps at the filler/matrix interfaces, the mixed-matrix carbon molecular sieve membrane (Matrimid®/H-zeolite 5A–30%) is still able to surpass the 2008 Robeson upper bound limit. Using a different benchmark, the hierarchical zeolite 5A filler at 30 wt% loading is also deemed "competent" based upon our analysis of a recently developed filler enhancement index. Taken altogether, our strategy is both more cost-effective and less sophisticated in approach. In this regard, our mixed-matrix carbon molecular sieve membranes offer greater competitive advantages when compared to other carbon molecular sieve membranes such as those derived from high-permeable polymers like 6FDA-based and PIM-1 polymers. Again, this demonstrate that our strategy holds promise in realizing high-performance membranes for CO_2/CH_4 separation.

Acknowledgement

This research is supported by the National Research Foundation, Prime Minister's Office, Singapore, and the National Environment Agency - Singapore, Ministry of the Environment and Water Resources - Singapore, under the Waste-to-Energy Competitive Research Programme (WTE CRP 1601 105). T. -H. Bae would like to thank KAIST for the financial support.

Appendix A. Supplementary data

Supplementary data to this article can be found online at https://doi.org/10.1016/j.memsci.2019.117220.

References

[1] A. Petersson, A. WeLLInGer, Biogas upgrading technologies–developments and innovations, IEA Bioenergy 20 (2009) 1–19.
[2] K. Ghosal, B.D. Freeman, Gas separation using polymer membranes: an overview,

Polym. Adv. Technol. 5 (1994) 673–697.
[3] G. Maier, Gas separation with polymer membranes, Angew. Chem. Int. Ed. 37 (1998) 2960–2974.
[4] C.A. Scholes, G.W. Stevens, S.E. Kentish, Membrane gas separation applications in natural gas processing, Fuel 96 (2012) 15–28.
[5] R.W. Baker, K. Lokhandwala, Natural gas processing with membranes: an overview, Ind. Eng. Chem. Res. 47 (2008) 2109–2121.
[6] S. Basu, A.L. Khan, A. Cano-Odena, C. Liu, I.F. Vankelecom, Membrane-based technologies for biogas separations, Chem. Soc. Rev. 39 (2010) 750–768.
[7] D. Bastani, N. Esmaeili, M. Asadollahi, Polymeric mixed matrix membranes containing zeolites as a filler for gas separation applications: a review, J. Ind. Eng. Chem. 19 (2013) 375–393.
[8] L.M. Robeson, The upper bound revisited, J. Membr. Sci. 320 (2008) 390–400.
[9] N. Jusoh, Y.F. Yeong, T.L. Chew, K.K. Lau, A.M. Shariff, Current development and challenges of mixed matrix membranes for CO_2/CH_4 separation, Separ. Purif. Rev. 45 (2016) 321–344.
[10] H.B. Park, C.H. Jung, Y.M. Lee, A.J. Hill, S.J. Pas, S.T. Mudie, E. Van Wagner, B.D. Freeman, D.J. Cookson, Polymers with cavities tuned for fast selective transport of small molecules and ions, Science 318 (2007) 254–258.
[11] R. Swaidan, X. Ma, E. Litwiller, I. Pinnau, High pressure pure- and mixed-gas separation of CO_2/CH_4 by thermally-rearranged and carbon molecular sieve membranes derived from a polyimide of intrinsic microporosity, J. Membr. Sci. 447 (2013) 387–394.
[12] Y. Zhang, J. Sunarso, S. Liu, R. Wang, Current status and development of membranes for CO_2/CH_4 separation: a review, Int. J. Greenh. Gas Con. 12 (2013) 84–107.
[13] W.N.W. Salleh, A.F. Ismail, T. Matsuura, M.S. Abdullah, Precursor selection and process conditions in the preparation of carbon membrane for gas separation: a review, Separ. Purif. Rev. 40 (2011) 261–311.
[14] W.N.W. Salleh, A.F. Ismail, Effects of carbonization heating rate on CO2 separation of derived carbon membranes, Separ. Purif. Technol. 88 (2012) 174–183.
[15] H. Gong, C.Y. Chuah, Y. Yang, T.-H. Bae, High performance composite membranes comprising $Zn(pyrz)_2(SiF_6)$ nanocrystals for CO_2/CH_4 separation, J. Ind. Eng. Chem. 60 (2018) 279–285.
[16] P.S. Goh, A.F. Ismail, S.M. Sanip, B.C. Ng, M. Aziz, Recent advances of inorganic fillers in mixed matrix membrane for gas separation, Separ. Purif. Technol. 81 (2011) 243–264.
[17] Z. Bing, S. Yi, Y. Wu, T. Wang, J. Qiu, Towards the preparation of ordered mesoporous carbon/carbon composite membranes for gas separation, Separ. Sci. Technol. 49 (2014) 171–178.
[18] L. Li, T. Wang, Q. Liu, Y. Cao, J. Qiu, A high CO_2 permselective mesoporous silica/carbon composite membrane for CO_2 separation, Carbon 50 (2012) 5186–5195.
[19] X. Yin, N. Chu, J. Yang, J. Wang, Z. Li, Thin zeolite T/carbon composite membranes supported on the porous alumina tubes for CO_2 separation, Int. J. Greenh. Gas Con. 15 (2013) 55–64.
[20] P.S. Tin, T.-S. Chung, L. Jiang, S. Kulprathipanja, Carbon–zeolite composite membranes for gas separation, Carbon 43 (2005) 2025–2027.
[21] X. Yin, J. Wang, N. Chu, J. Yang, J. Lu, Y. Zhang, D. Yin, Zeolite L/carbon nanocomposite membranes on the porous alumina tubes and their gas separation properties, J. Membr. Sci. 348 (2010) 181–189.
[22] C. Duan, X. Jie, H. Zhu, D. Liu, W. Peng, Y. Cao, Gas-permeation performance of metal organic framework/polyimide mixed-matrix membranes and additional explanation from the particle size angle, J. Appl. Polym. Sci. 135 (2018) 45728.
[23] Y. Li, H.-M. Guan, T.-S. Chung, S. Kulprathipanja, Effects of novel silane modification of zeolite surface on polymer chain rigidification and partial pore blockage in polyethersulfone (PES)–zeolite A mixed matrix membranes, J. Membr. Sci. 275 (2006) 17–28.
[24] Y. Li, T.-S. Chung, C. Cao, S. Kulprathipanja, The effects of polymer chain rigidification, zeolite pore size and pore blockage on polyethersulfone (PES)-zeolite A mixed matrix membranes, J. Membr. Sci. 260 (2005) 45–55.
[25] O. Bakhtiari, S. Mosleh, T. Khosravi, T. Mohammadi, Preparation, characterization and gas permeation of polyimide mixed matrix membranes, J. Membr. Sci. Technol. 1 (2011) 1–6.
[26] D. Sen, H. Kalipcilar, L. Yilmaz, Development of zeolite filled polycarbonate mixed matrix gas separation membranes, Desalination 200 (2006) 222–224.
[27] C.Y. Chuah, K. Goh, Y. Yang, H. Gong, W. Li, H.E. Karahan, M.D. Guiver, R. Wang, T.-H. Bae, Harnessing filler materials for enhancing biogas separation membranes, Chem. Rev. 118 (2018) 8655–8769.
[28] T.H. Nguyen, S. Kim, M. Yoon, T.H. Bae, Hierarchical zeolites with amine-functionalized mesoporous domains for carbon dioxide capture, ChemSusChem 9 (2016) 455–461.
[29] W. Li, S. Samarasinghe, T.-H. Bae, Enhancing CO_2/CH_4 separation performance and mechanical strength of mixed-matrix membrane via combined use of graphene oxide and ZIF-8, J. Ind. Eng. Chem. 67 (2018) 156–163.
[30] T.H. Bae, J.S. Lee, W. Qiu, W.J. Koros, C.W. Jones, S. Nair, A high-performance gas-separation membrane containing submicrometer-sized metal–organic framework crystals, Angew. Chem. Int. Ed. 49 (2010) 9863–9866.
[31] N. Prasetya, A.A. Teck, B.P. Ladewig, Matrimid-JUC-62 and Matrimid-PCN-250 mixed matrix membranes displaying light-responsive gas separation and beneficial ageing characteristics for CO_2/N_2 separation, Sci. Rep. 8 (2018) 2944.
[32] H. Gong, S.S. Lee, T.-H. Bae, Mixed-matrix membranes containing inorganically surface-modified 5A zeolite for enhanced CO_2/CH_4 separation, Microporous Mesoporous Mater. 237 (2017) 82–89.
[33] T.-H. Bae, J. Liu, J.A. Thompson, W.J. Koros, C.W. Jones, S. Nair, Solvothermal deposition and characterization of magnesium hydroxide nanostructures on zeolite crystals, Microporous Mesoporous Mater. 139 (2011) 120–129.
[34] C.Y. Chuah, S. Yu, K. Na, T.-H. Bae, Enhanced SF6 recovery by hierarchically structured MFI zeolite, J. Ind. Eng. Chem. 62 (2018) 64–71.
[35] M. Calle, Y.M. Lee, Thermally rearranged (TR) poly (ether− benzoxazole) membranes for gas separation, Macromolecules 44 (2011) 1156–1165.
[36] S.H. Han, N. Misdan, S. Kim, C.M. Doherty, A.J. Hill, Y.M. Lee, Thermally rearranged (TR) polybenzoxazole: effects of diverse imidization routes on physical properties and gas transport behaviors, Macromolecules 43 (2010) 7657–7667.
[37] F. Weigelt, P. Georgopanos, S. Shishatskiy, V. Filiz, T. Brinkmann, V. Abetz, Development and characterization of defect-free Matrimid® mixed-matrix membranes containing activated carbon particles for gas separation, Polymers 10 (2018) 51.
[38] M. Yoshimune, K. Haraya, Flexible carbon hollow fiber membranes derived from sulfonated poly(phenylene oxide), Separ. Purif. Technol. 75 (2010) 193–197.
[39] A.F. Ismail, L. David, A review on the latest development of carbon membranes for gas separation, J. Membr. Sci. 193 (2001) 1–18.
[40] A. Fuertes, D. Nevskaia, T. Centeno, Carbon composite membranes from Matrimid® and Kapton® polyimides for gas separation, Microporous Mesoporous Mater. 33 (1999) 115–125.
[41] Y. Xiao, Y. Dai, T.-S. Chung, M.D. Guiver, Effects of brominating Matrimid polyimide on the physical and gas transport properties of derived carbon membranes, Macromolecules 38 (2005) 10042–10049.
[42] E. Favvas, G. Kapantaidakis, J. Nolan, A.C. Mitropoulos, N. Kanellopoulos, Preparation, characterization and gas permeation properties of carbon hollow fiber membranes based on Matrimid® 5218 precursor, J. Mater. Process. Technol. 186 (2007) 102–110.
[43] A.K. Itta, H.-H. Tseng, M.-Y. Wey, Effect of dry/wet-phase inversion method on fabricating polyetherimide-derived CMS membrane for H_2/N_2 separation, Int. J. Hydrogen Energy 35 (2010) 1650–1658.
[44] W. Wei, G. Qin, H. Hu, L. You, G. Chen, Preparation of supported carbon molecular sieve membrane from novolac phenol–formaldehyde resin, J. Membr. Sci. 303 (2007) 80–85.
[45] T.A. Centeno, J.L. Vilas, A.B. Fuertes, Effects of phenolic resin pyrolysis conditions on carbon membrane performance for gas separation, J. Membr. Sci. 228 (2004) 45–54.
[46] M. Kiyono, P.J. Williams, W.J. Koros, Effect of pyrolysis atmosphere on separation performance of carbon molecular sieve membranes, J. Membr. Sci. 359 (2010) 2–10.
[47] A. Fuertes, T. Centeno, Preparation of supported asymmetric carbon molecular sieve membranes, J. Membr. Sci. 144 (1998) 105–111.